Microscopic study of carbon surfaces interacting with high carbon ferromanganese slag

Jafar Safarian*, Leiv Kolbeinsen**

* SINTEF Materials and Chemistry, Alfred Getz Vei 2, 7465 Trondheim, Norway,

**Norwegian University of Science and Technology, Alfred Getz Vei 2, 7491 Trondheim, Norway

Abstract

The interaction of carbon materials with molten slags occurs in many pyro-metallurgical processes. In the production of high carbon ferromanganese in submerged arc furnace, the carbothermic reduction of MnO-containing silicate slags yields the metal product. In order to study the interaction of carbon with MnO containing slags, sessile drop wettability technique is employed in this study to reduce MnO from a molten slag drop by carbon substrates. The interfacial area on the carbon substrate before and after reaction with slag is studied by scanning electron microscope. It is indicated that no Mn metal particles are found at the interface through the reduction of the MnO slag. Moreover, the reduction of MnO occurs through the contribution of Boudouard reaction and it causes carbon consumption in particular active sites at the interface, which generate carbon degradation and open pore growth at the interface. It is shown that the slag is fragmented to many micro-droplets at the reaction interface, potentially due to the effect on the interfacial energies of a provisional liquid Mn thin film. The rapid reduction of these slag micro-droplets affects the carbon surface with making deep micro-pores. A mechanism for the formation of slag micro-droplets is proposed, which is based on the formation of provisional micro thin films of liquid Mn at the interface.

Key words: *Carbon, Slag, Interface, carbothermic, reduction, sessile drop,*

1. Introduction

High carbon ferromanganese (HCFeMn) is commonly produced in submerged arc furnace. In this process, manganese oxides in the form of lump ore, sinter, etc. are generally reduced to MnO directly by CO gas. In the coke bed area of the furnace, where the process heat is generated by graphite electrodes, manganese is mainly produced through the interaction of a high MnO-containing silicate slag with carbon:

$$(MnO) + C\ (s) = Mn\ (l) + CO\ (g) \qquad \Delta G^{\circ}_{(1300\text{-}1800^{\circ}C)} = 288\text{-}0.17T \quad kJ \qquad (1)$$

The kinetic and mechanism of carbothermic reduction of MnO by different graphite materials was studied previously [1)] and it was found that the wettability of graphite by HCFeMn slag is not good and contact angles around 150° were measured. The type of carbon substrate and the gas phase composition are both affecting the kinetics of MnO reduction[2,3)]. If there is FeO in the slag, this is reduced initially and then a FeMn alloy is produced through further MnO reduction.[4] If the initial slag does not contain FeO, the produced Mn through the carbothermic reduction is rapidly evaporated due to the high vapor pressure of Mn at elevated temperatures as described in our previous work[1)].

In the present study, the interfacial contact area between carbon substrates with different carbon qualities and a MnO-containing slag is studied through microscopic examination. In this case a MnO-containing silicate slag and without FeO is reduced. Since no stable liquid metallic phase can grow at the interface and the wetting of the carbon by slag is weak, the slag

drop does not stick to the carbon substrate. This is advantageous and makes it possible to study the interfacial contact area on the carbon substrate surface.

2. Methodology

A synthetic slag was made from high purity (+99.99%) fine powders of CaO, MgO, SiO_2 and Al_2O_3 with ratio of CaO/MgO=2, CaO/Al_2O_3=1.34 and Al_2O_3/SiO_2=0.4. The powders were mixed in a ball mill and the mixture was melted in a graphite crucible in air using an induction furnace. The obtained slag was crushed in a tungsten carbide disc mill to a very fine powder with size of 80% under 45 microns and was then mixed with appropriate amounts of high purity MnO (+99.95%) fine powder by hand in plastic containers. The obtained mixture was melted in a platinum crucible in air at 1550°C and the slag composition was measured by Electron Probe Micro-Analysis (EPMA) supported by Wavelength Dispersive Spectroscopy (WDS). The slag composition was 45%MnO-3.4%CaO-25%SiO_2-10%Al_2O_3-6.6%MgO.

Two different carbon materials were used in the present study; graphite and glassy carbon. The graphite was cut from a graphite block and two different surfaces of this material were prepared, a rough surface obtained through cutting and a polished surface made with 4000 emery paper. The measured roughness for the cut graphite surface was 3.41 μm, while it was 0.2 μm for the polished one. A glassy carbon with two surface qualities; rough surface and mirror surface, were also used in the present work.

Sessile drop wettability technique was used in order to study the interaction between the synthetic slag and the carbon substrates. A schematic diagram of the experimental set up is shown in Fig. 1. The carbon substrate was located in the graphite sample holder and a 40±1

mg slag particle was put on the carbon surface. The furnace chamber was evacuated initially, and then the furnace was heated slowly in pure argon (99.9999%Ar) with 0.5 Nl/min flow rate. The furnace was heated to 950°C in approximately 10 minutes, followed by a rapid heating rate of 120°C/min to 1500°C or 1600°C. At these temperatures reaction periods of 30 or 60 minutes were followed by rapid cooling. For the cut graphite surface, the experiment was done in both temperatures and for the other carbon surfaces only at 1600°C. The temperature was controlled using a Keller PZ40 two color pyrometer (Keller, GMBH, Ibbenburen, Germany) focused on the edge of the graphite sample holder.

After completion of the experiments, the reacted slag droplet and carbon substrates were separated due to no sticking between them, as expected. The surface of the reacted carbon before and after reaction was studied by Scanning Electron Microscope (SEM) supported with Energy Dispersive Spectroscopy (EDS).

3. Results

The results of microscopic study of the contacted carbon surfaces with the slag drop are presented as follows.

3.1 Graphite surface

The cut surface of the graphite substrate before and after reaction with the slag at 1500°C is shown in Figure 2. As seen, the number and size of the pores inside the slag-carbon contact area is increased after reaction, and also relative to the area outside the contact area (images 2-a and 2-b). Microscopic study of the graphite surface in the reacted area also shows the existence of many micro-droplets of the slag as illustrated in images 2-c to 2-f. These micro-

droplets are sitting around the surface pores, namely the areas that are most likely to be in physical contact with the slag drop. Two types of micro-droplets were observed with regard to the EDS analysis results. Figure 3 indicates that some of them contain Mn (most likely larger particles), while the majority of them do not contain Mn.

Figure 4 shows images of the reacted area on the cut graphite surface at 1600 °C after 30 minutes reaction. As we see, almost identical observations as with the graphite reacted at 1500 °C can be observed. However, one important difference is that graphite consumption at the contact area at 1600 °C (image 4-a) is more uniform than 1500 °C (image 2-b) so that there are less visible surface pores and the graphite has been consumed more uniformly in the all contact area. Moreover, the micro-droplets have more affected the carbon substrate around and they have penetrated into the surface. This observation may indicate that the slag is more aggressive to carbon at 1600°C, compared to 1500°C. The analysis of the micro-droplets indicated that they are all almost free of Mn for the reaction at 1600 °C.

Figure 5 shows SEM images from the contact area of the polished graphite surface after 30 minutes reaction at 1600 °C. The polished graphite has reacted much less with the slag compared to the cut graphite surface as observed clearly through comparing Figures 4 and 5. Moreover, slag micro-droplets are again observed on the graphite surface and deep cylindrical pores are formed through their interaction with the graphite. However, there are much fewer slag micro-droplets on the polished graphite surface compared to that on the reacted cut surface.

3.2 Glassy carbon surface

Figure 6 shows the rough surface of glassy carbon, image *(a)* shows the whole contact area at low magnification, and it indicates low carbon consumption, compared to the graphite substrate surfaces. Image *(b)* is from the un-reacted area and it shows that the rough carbon surface contains small closed surface pores. The comparison of the reacted surface in image (c) with image (b) reveals that carbon has been consumed on the surface inside the pores so that the pore walls are rougher than the pores in un-reacted surface. Moreover, numerous micro-droplets are found around the surface pores, the areas most likely in better contact with the main slag drop. Obviously, the micro-droplets have affected the carbon surface significantly and penetration of the micro-droplets into the substrate is observed.

Figure 7 shows the mirror surface of the glassy carbon after reaction. It indicates a completely different contact area between the slag drop and the substrate (image 7-*a*), compared to the rough surface (Figure 6). As we see the carbon substrate has reacted mainly in a belt zone around the contact area, and we see almost not reacted carbon in a large part of the contact area. Obviously, the reaction has been occurred at the slag/carbon/gas interface. Image *(a)* shows that the contact area is not circular. This is due to a little displacement of the slag drop during the reduction, the drop movement was also observed during the experiment. Image 7-b illustrates the reacted belt zone area at high magnification. Comparing both sides of the belt zone area, no significant carbon reaction is observed inside of the slag-carbon contact area, and the surface is similar to the un-reacted area far away from the slag drop. Regarding the slag reduction and accordingly decreased slag volume, the initial slag/carbon/gas interface is on the left side of the belt zone in image 7-b, and when the reaction is stopped, it is on the right side of this area. Therefore, we may say that the reacted carbon surface structure in the belt zone has been created during the reduction.

4. Discussion

With regard to the above observations for the interaction of carbon and slag, thermochemistry of the system, and literature the obtained results are discussed as follows to clarify more details about the carbon-slag reaction.

4.1 Carbon gasification at the interface

It was observed that the surface pores are formed on the carbon in the interfacial area between the slag drop and the substrate. The formation of larger pores is clearer at lower temperature as observed for graphite at 1500°C compared to it at 1600°C. When polished graphite and mirror glassy carbon surfaces were interacted with the slag, less carbon consumption was observed compared to their rough surfaces. These observations can be explained by considering chemically active carbon sites on the substrate surface, the contribution of Boudouard reaction in the slag reduction, and fast evaporation of the metal products.

The carbothermic reduction of MnO in the slag according to reaction (1) is initiated at some active carbon sites at the interface. These chemically active sites are most likely at the edges of the open pores on the carbon surface as schematically shown in Figure 8. Based on the thermodynamics of the system at high temperatures the following reactions take place at the interface simultaneous with the reaction (1):

$$Mn\ (l) = Mn\ (g) \qquad (2)$$

$$(MnO) + CO\ (g) = Mn + CO_2\ (g) \qquad (3)$$

Observing no Mn metal at the interface confirms that reaction (2) occur at the interface as discussed previously[1]. The produced CO_2 through reaction (3) at the interface is further reacted with the carbon in the pore walls according to the Boudouard reaction:

$$CO_2\ (g) + C = 2CO\ (g) \qquad (4)$$

Reaction (4) is favorable as written at elevated temperatures and the surface pores become larger through this reaction as clearly seen in Figure 2. This carbon gasification phenomenon is schematically shown in Figures 8-a to 8-c. The slag reduction mechanism and carbon mass transport route between the substrate and slag is schematically illustrated in Figure 8.d. As seen, there is a gas phase between the carbon and condensed slag phases and we have a counter current flow of CO and CO_2 components in the gas phase giving a net mass flow of carbon away from the carbon surface. When the slag-carbon interaction occurs at higher temperature, more chemically active sites on the carbon surface may initiate the slag reduction and therefore they cause higher number of pores to grow and consequently more uniform carbon gasification at the interface. The Boudouard reaction (4) is also faster at higher temperatures and intensifies the carbon consumption at interface. Both these factors may led to the more uniform carbon gasification at the interface at 1600°C compared to 1500°C as clearly seen in Figures 2-b and 4-a.

The consumption of carbon at the slag-substrate interfacial area is affected by the surface roughness of the substrate. When smoother carbon surfaces are reacted with the slag, the number of active sites on the carbon surface is very limited compared to the reaction with rough carbon surfaces. This is the main reason for observing less carbon consumption for the polished graphite than for the cut graphite under the same reaction conditions as seen clearly

in Figures 4 and 5. The mirror surface of the glassy carbon is also less reactive than the rough surface and therefore it shows much less interaction with the slag. Obviously, the most favorable place for the chemical reduction reactions is the slag-carbon-gas interfacial area for the mirror glassy carbon surface, which is a belt zone around the slag drop. Since the gaseous products from the reduction and evaporation c reactions are rapidly transported to the bulk gas phase from this three-phase contact area, may also cause the reactions in this area to be more favorable. Therefore, the slag reduction is initiated in a circular area over the carbon surface, and with further reduction it creates the observed surface morphology on the mirror surface of the glassy carbon (Figure 7). When the rough surface of the glassy carbon is contacted with the slag, there are many active sites in the whole contact area due to the rough surface morphology and this causes carbon consumption in the whole contact area and also surface pore growth through the above mentioned mechanism which causes the carbon gasification as seen in Figure 6.

4.2 Slag fragmentation to micro-droplets

The microscopic examination indicated that there are no slag micro-droplets in the surface pores, while they are located around the pores, the areas that there are in better contact with the main slag drop. Two types of slag micro-droplets were found on the interface; Mn-containing and Mn-free micro-droplets. Since the Mn-containing droplets were observed for only the sample reacted at lower temperature (1500 °C), we may say that MnO reduction from these droplets has not been completed. In contrast, it has been completed in the micro-droplets at 1600 °C due to the faster reduction rate. The reduction of MnO from the micro-droplets is faster than the main slag drop due to better contact with the carbon substrate and also their much larger surface to volume ratio. Hence, we may argue that the separation of the micro-droplets from the main slag drop is a physical separation and they are rapidly reduced after

the separation. This physical separation cannot be easily explained due to the creation of new slag-gas interfacial area, which has high interfacial energy.[5] Therefore, we may consider the role of the chemical reactions and other phases which may facilitate this phenomenon.

The mechanism of the slag micro-droplets formation from the main slag drop at the slag-carbon interface can be explained through the provisional formation of a thin film of liquid Mn at some active locations at the interface. When MnO reduction occurs at these sites the produced liquid Mn is simultaneously evaporated. Since, there is no rapid mass transport path for the evaporated Mn to leave the interface, this interfacial area becomes saturated of Mn vapour and therefore a thin film of liquid Mn can survive at the interface for a while. The formation of this liquid Mn thin film is schematically shown in Figure 9-a and 9-b. Regarding the good wetting of carbon with liquid Mn and the low interfacial tension between the liquid Mn and the slag[6] , this liquid thin film gets proper contact with these solid and liquid phases as shown in Figure 9-b. This liquid film may move down or even drag a part of the slag to the carbon interface (Figure 9-c), while reduction reactions are taking place. It is worth mentioning that MnO reduction from the slag at this area can even occur with the dissolved carbon in the liquid metal, which is expected to be very fast. Both the minimization of the interfacial energies and chemical reaction energies may cause the separation of a micro-droplet from the main drop by the aid of the metal thin film as illustrated in Figure 9-d. The liquid metal thin film vanishes after a while, when Mn evaporation rate becomes higher than the Mn production rate, and the reduction of the slag micro-droplet is being continues by the surrounding solid carbon according to the above described mechanism. This will finally create a deep micro-pore and a slag micro-droplet low or free of MnO. Observing no slag micro-droplet in the large surface pores supports this mechanism due to the lack of possible formation of liquid Mn thin film in the large surface pores. This is related to Mn vapour

unsaturation and also lack of enough liquid Mn to make a continuous liquid thin film on the pore wall.

5. Conclusions

The interaction of high carbon ferromanganese slag with carbon substrates with different surface properties was studied through sessile drop wettability technique. A method for studying slag-carbon interaction at elevated temperatures through electron microscopy examination was applied. The main conclusions of the present work can be summarized as:

- The carbothermic reduction of MnO rich slag takes place through the contribution of Boudouard reaction which causes carbon gasification, carbon surface degradation, and open pore growth at the reaction interface.
- It is proposed that the carbothermic reduction reactions are initiated in reactive carbon sites; the number of these sites is increased with increasing the surface roughness and temperature.
- The slag fragmentation into slag micro-droplets at the interfacial areas between the surface pores of carbon takes place through the slag-carbon interaction; these micro-droplets react rapidly with the carbon substrate and they affect the morphology of the carbon surface
- It is proposed that a liquid thin film of manganese at the interfacial area between the slag and carbon plays an important role for the separation of slag micro-droplets from the slag and it can even contribute in the reactions.
- Possible future attempts in atomistic level modelling of these reactions, including their thermodynamics, reaction kinetics and the involved transport phenomena may reveal if the explanations and conclusions set forward here are viable or not.

Figure captions

Figure 1: Schematic of the sessile drop wettability set up (a), and a photograph taken from the slag drop and carbon substrate (b).

Figure 2: The SEM images from the cut graphite surface before and after reaction with the slag at 1500° C for one hour. (*a*): Un-reacted surface, (*b*): Low magnification image from the whole slag-carbon contact area, (*c*): reacted surface in the middle of contact area, (*d*): both unreacted area (right) and reacted area (left), (*e*): very small grey particles in the contact area, (*f*): a pore in the contact area. Note: the magnifications of the images are not the same.

Figure 3: The EDS spectrums of the particles on the contact area of graphite substrate. (a): larger particles, (b): smaller particles.

Figure 4: The SEM images from the cut graphite surface after reaction with slag at 1600 °C for 30 min. *(a)*: The whole contact area, *(b)*: Un-reacted surface (right) and the slag-carbon contact area (left, *(c)*: Slag micro-droplets in the slag-carbon contact area in high magnification.

Figure 5: The SEM images from the surface of polished graphite C after interaction with slag drop at 1600 °C for 30 minutes *(a)*: the reacted surface (up and right) and the un-reacted surface (down and left), *(b)*: the whole contact area, (c): high magnification image from the slag-carbon interfacial area.

Figure 6: SEM photographs from the glassy carbon rough surface reacted with slag at 1600°C for 30 minutes. *(a)*: the whole contact area, *(b)*: from the un-reacted surface, *(c)* and *(d)*: from the middle of slag-carbon contact area.

Figure 7: SEM photographs from the glassy carbon mirror surface reacted with slag at 1600°C for 30 minutes. *(a)*: the whole contact area, *(b)*: the belt zone area in image *(a) in higher magnification*.

Figure 8: Schematic of carbon gasification phenomenon and surface pore growth (a to c), and the mechanism of carbon gasification at the pore wall.

Figure 9: Schematic of the mechanism of slag micro-droplet separation and reaction with carbon substrate, (*a*): slag-carbon interaction in an active site at the interface, (*b*): Mn production, evaporation and liquid Mn thin film formation at the reacted carbon area, (*c*): Wetting improvement by the liquid metal film and slag drag toward the carbon, (*d*): separated liquid slag micro-droplet, (*e*): micro-droplet in contact with carbon after liquid Mn evaporation, (*f*): slag micro-droplet in a deep micro-pore after slag reduction.

References

1. J. Safarian, L. Kolbeinsen: ISIJ International, Vol. 48 (2008), No. 4, pp. 395–404.

2. J. Safarian, G. Tranell, L. Kolbeinsen, M. Tangstad, S. Gaal, J. Kaczorowski: Met. Mat. Trans. 39B (2008), 702-712.

3. M. Yastreboff, O. Ostrovski, and S. Ganguly: ISIJ Int., 2003, vol. 43 (2), pp. 161–65.

4. J. Safarian, L. Kolbeinsen, M. Tangstad, G. Tranell: Met. Mat. Trans. 40B (2009), 929-939.

5. T. M. Kekelidze, Sh. M. Mikiashvili, T. I. Dzhintsaradze, R. V. Khomeriki: Izv. AN. Gruz. SSR, Ser. Khim 4 (1878), 240.

6. J. Safarian, M. Tangstad: The 12th International Ferroalloys Congress, Helsinky, Finland, June 6-9, 2010, 327-337.

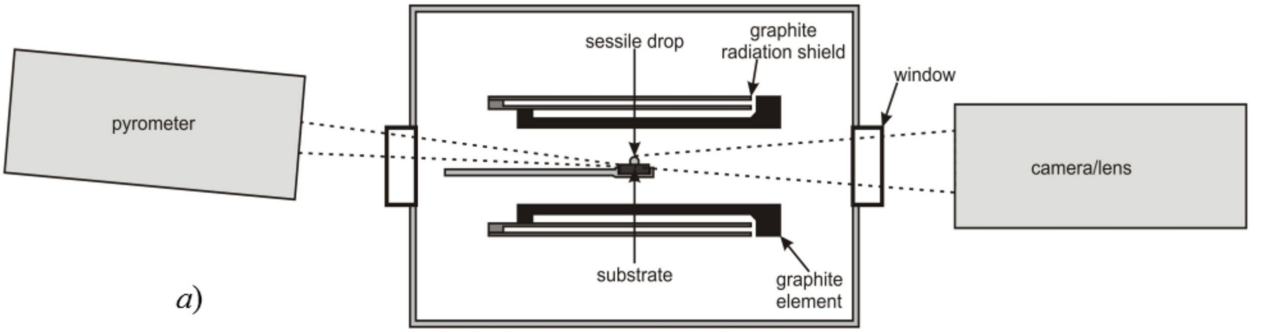

a)

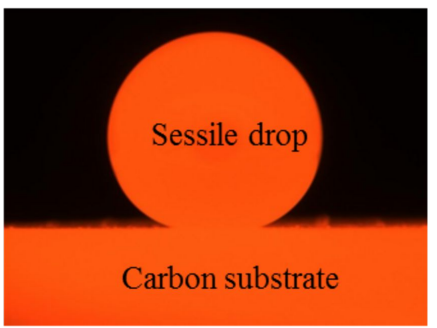

b)

Figure 1: Schematic of the sessile drop wettability set up (a), and a photograph taken from the slag drop and carbon substrate (b).

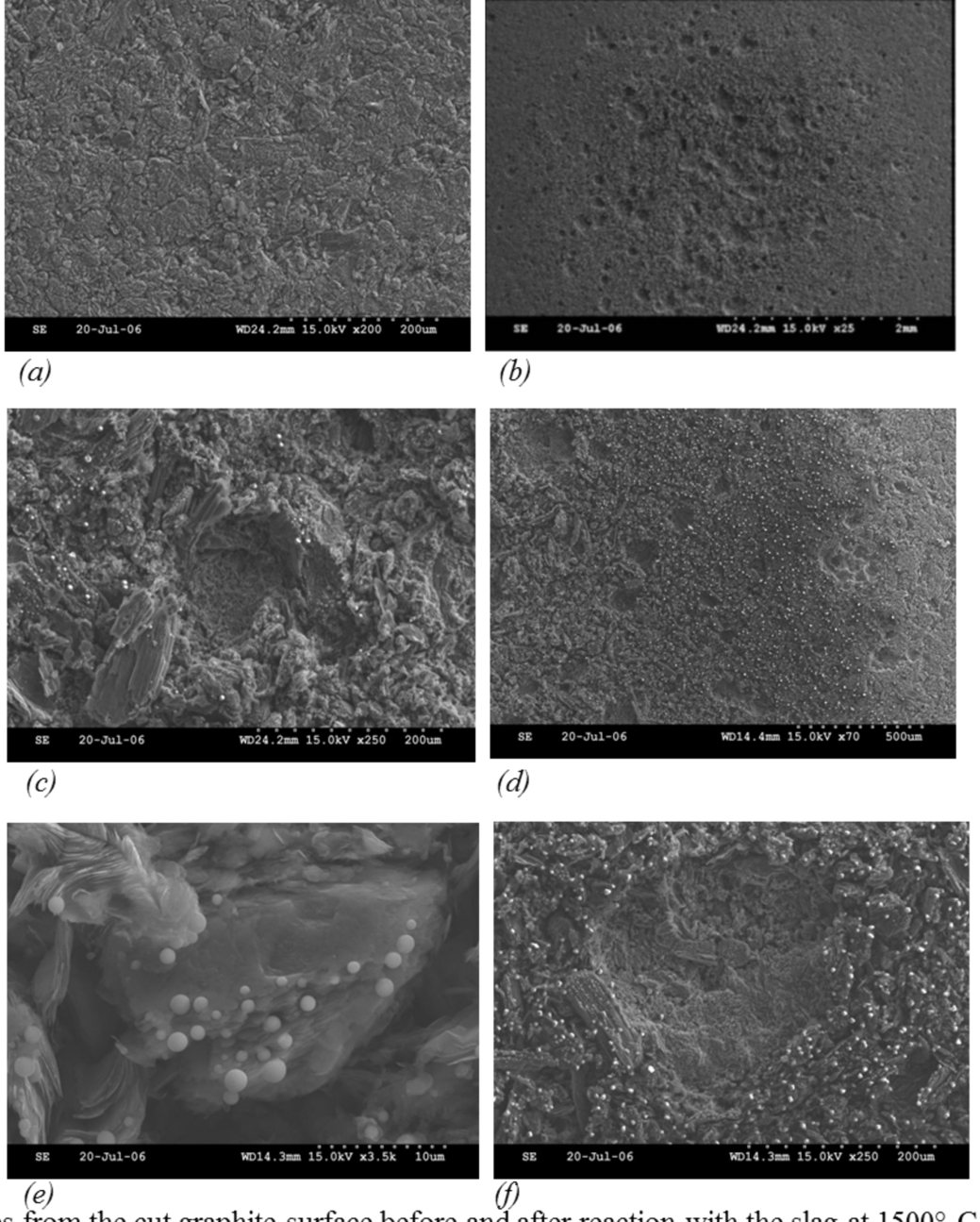

(a) *(b)* *(c)* *(d)* *(e)* *(f)*

Figure 2: The SEM images from the cut graphite surface before and after reaction with the slag at 1500° C for one hour. (*a*): Un-reacted surface, (*b*): Low magnification image from the whole slag-carbon contact area, (*c*): reacted surface in the middle of contact area, (*d*): both unreacted area (right) and reacted area (left), (*e*): very small grey particles in the contact area, (*f*): a pore in the contact area. Note: the magnifications of the images are not the same.

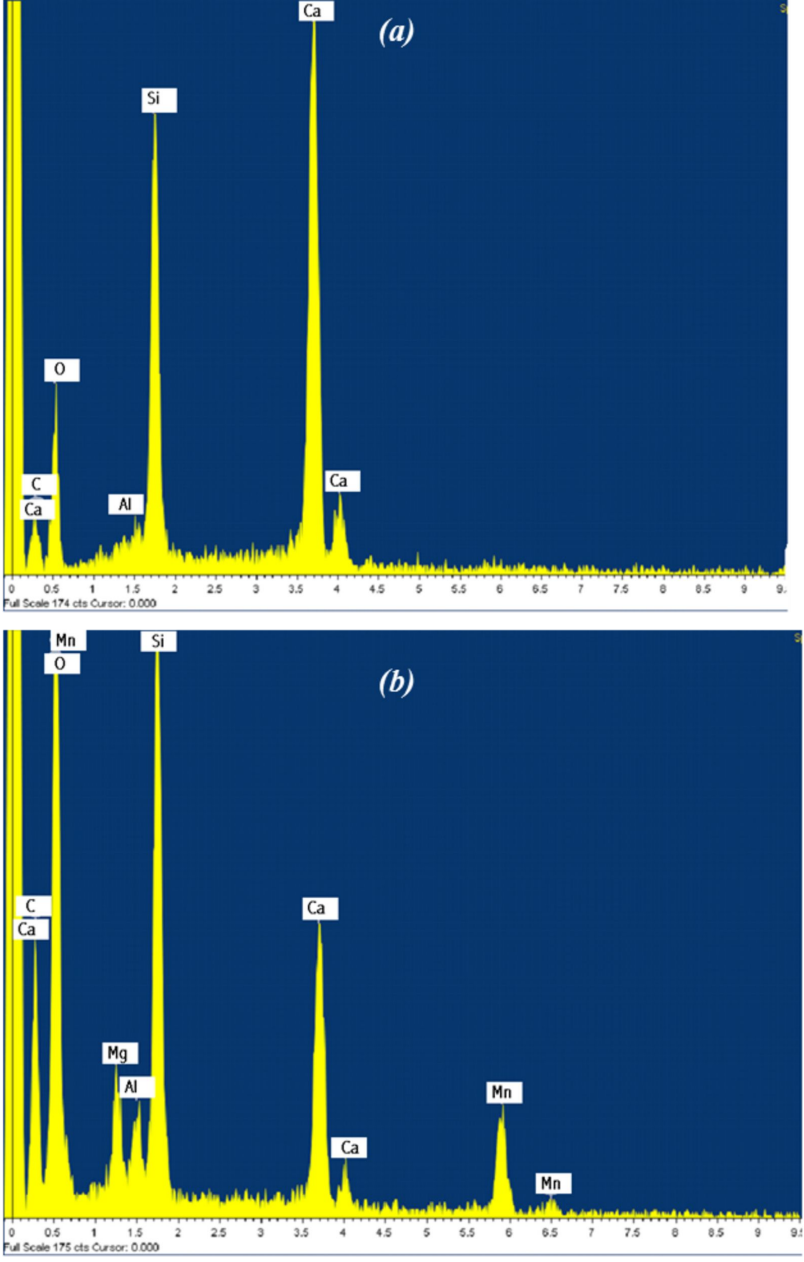

Figure 3: The EDS spectrums of the particles on the contact area of graphite substrate. (a): larger particles, (b): smaller particles.

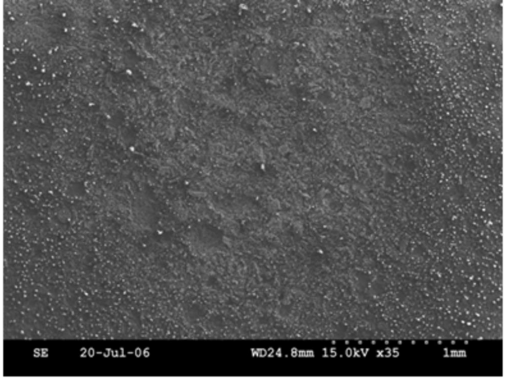

(a)

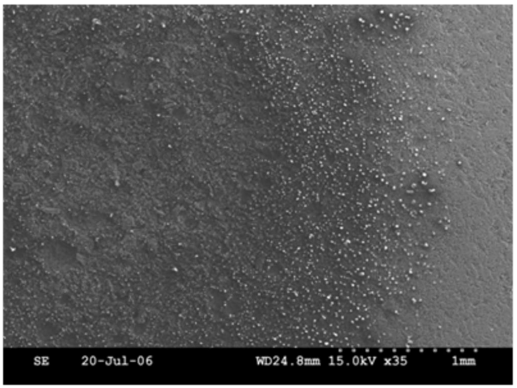

(b)

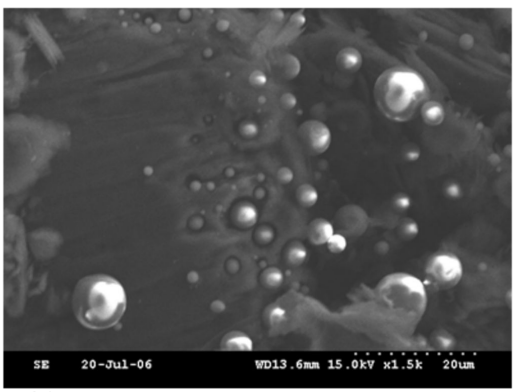

(c)

Figure 4: The SEM images from the cut graphite surface after reaction with slag at 1600 °C for 30 min. *(a)*: The whole contact area, *(b)*: Un-reacted surface (right) and the slag-carbon contact area (left, *(c)*: Slag micro-droplets in the slag-carbon contact area in high magnification.

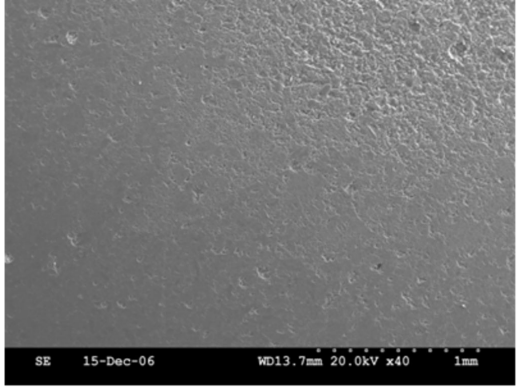

(a)

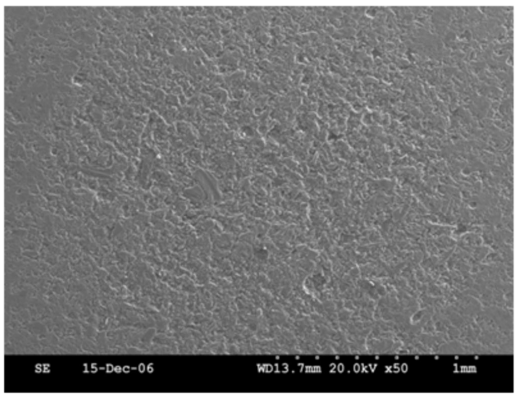

(b)

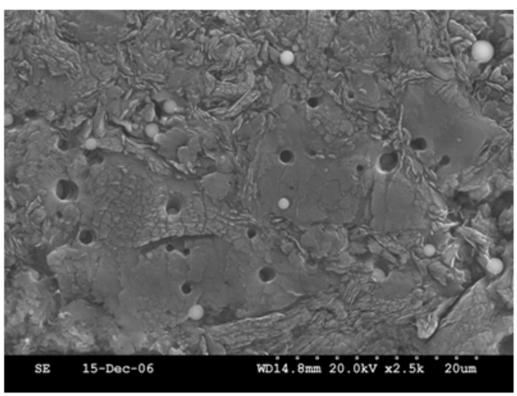

(c)

Figure 5: The SEM images from the surface of polished graphite C after interaction with slag drop at 1600 °C for 30 minutes *(a)*: the reacted surface (up and right) and the un-reacted surface (down and left), *(b)*: the whole contact area, (c): high magnification image from the slag-carbon interfacial area.

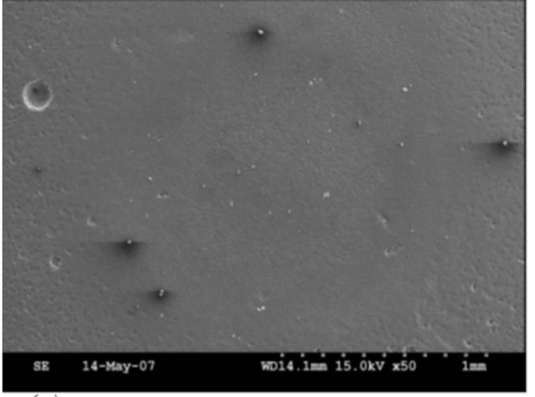

(a)

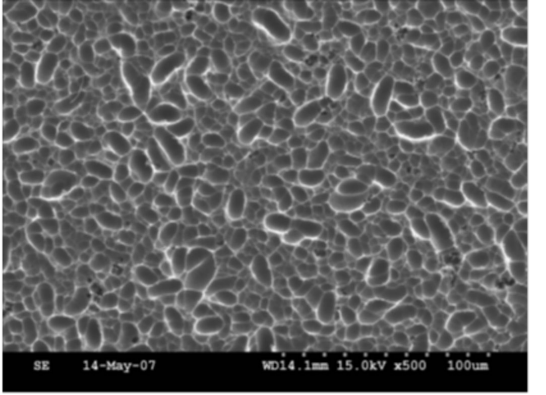

(b)

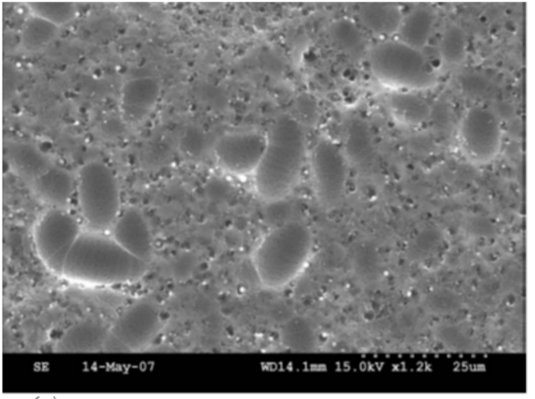

(c)

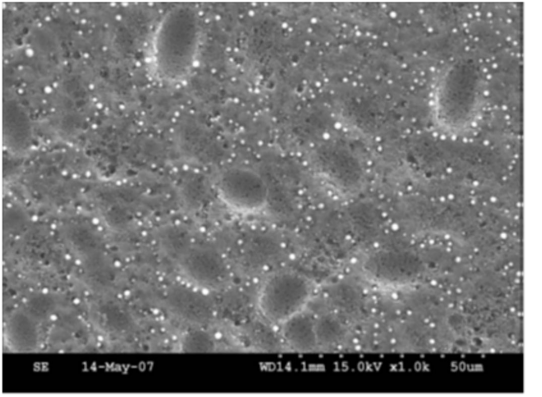

(d)

Figure 6: SEM photographs from the glassy carbon rough surface reacted with slag at 1600°C for 30 minutes. *(a)*: the whole contact area, *(b)*: from the un-reacted surface, *(c)* and *(d)*: from the middle of slag-carbon contact area.

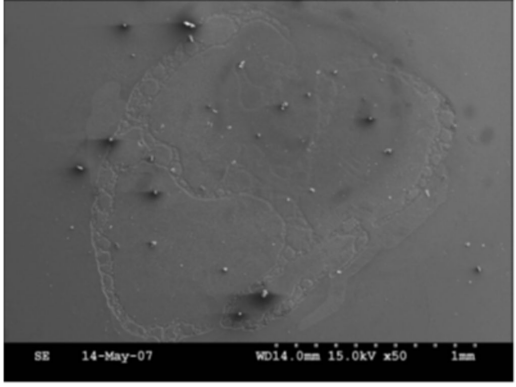

(a)

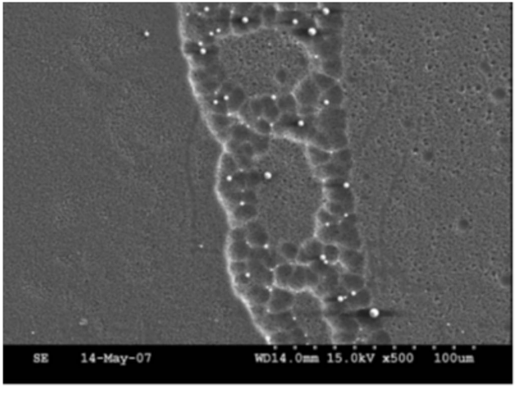

(b)

Figure 7: SEM photographs from the glassy carbon mirror surface reacted with slag at 1600°C for 30 minutes. *(a)*: the whole contact area, *(b)*: the belt zone area in image *(a) in higher magnification*.

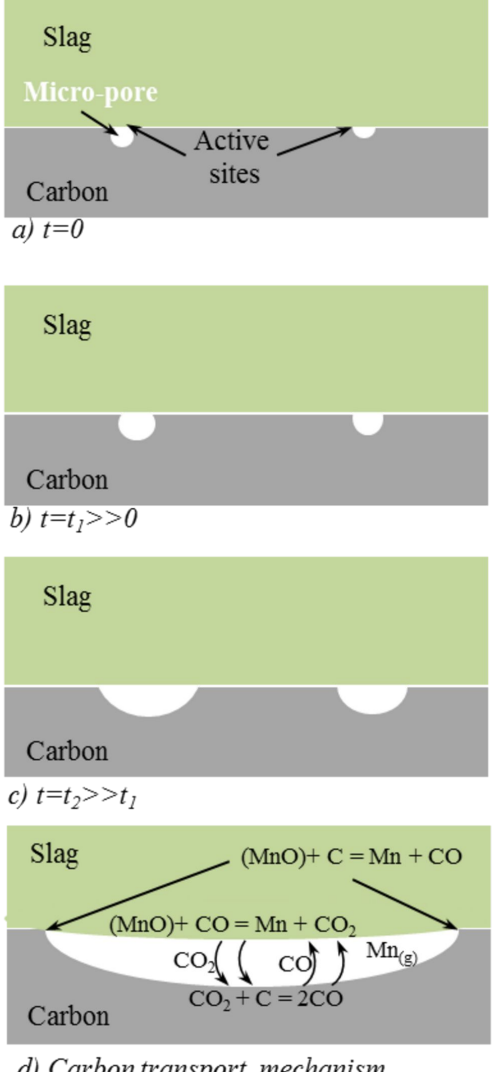

Figure 8: Schematic of carbon gasification phenomenon and surface pore growth (a to c), and the mechanism of carbon gasification at the pore wall.

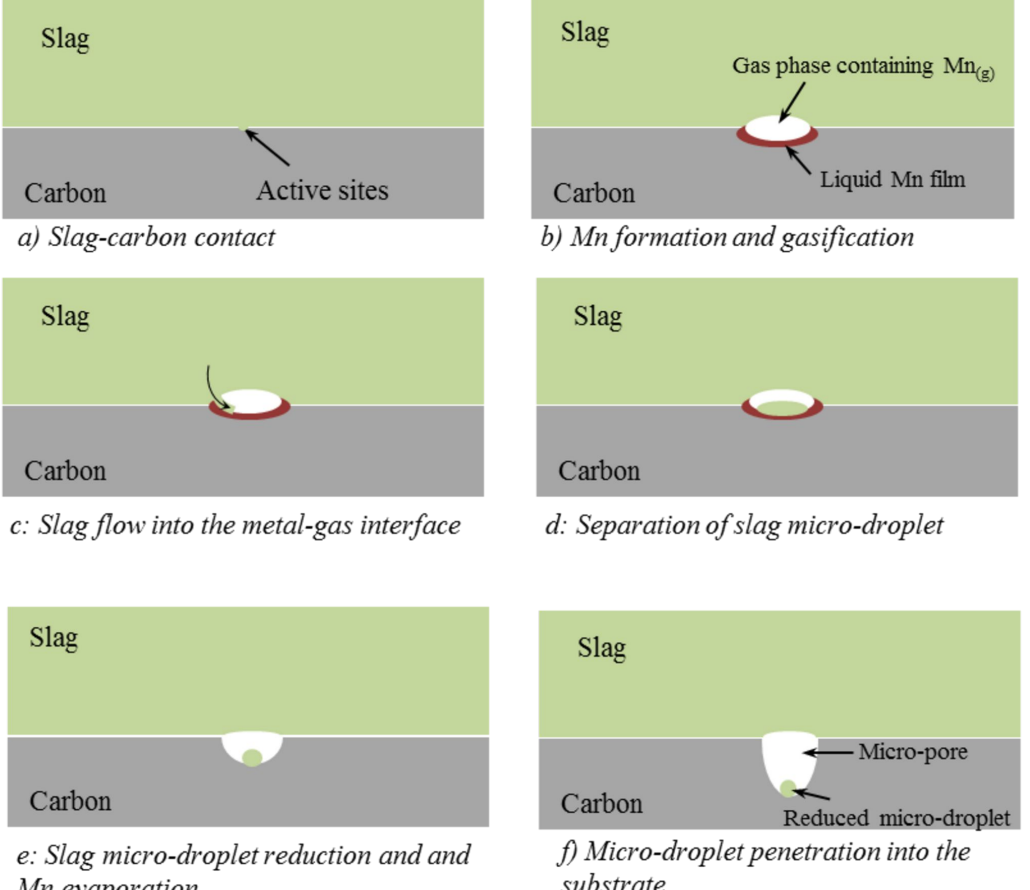

Figure 9: Schematic of the mechanism of slag micro-droplet separation and reaction with carbon substrate, (*a*): slag-carbon interaction in an active site at the interface, (*b*): Mn production, evaporation and liquid Mn thin film formation at the reacted carbon area, (*c*): Wetting improvement by the liquid metal film and slag drag toward the carbon, (*d*): separated liquid slag micro-droplet, (*e*): micro-droplet in contact with carbon after liquid Mn evaporation, (*f*): slag micro-droplet in a deep micro-pore after slag reduction.